Thermodynamics Drive Changes in the Antarctic Sea Ice Seasonal Cycle Following 2016

Kenza Himmich[1], Martin Vancoppenolle[1], Sharon Stammerjohn[2], Marion Bocquet[3,5], Gurvan Madec[1,4], Jean-Baptiste Sallée[1], Sara Fleury[3]

[1] Sorbonne Université, Laboratoire d'Océanographie et du Climat, CNRS/IRD/MNHN, Paris, France
[2] Institute of Arctic and Alpine Research, University of Colorado, Boulder, CO, 80309, USA
[3] LEGOS, Université de Toulouse, CNES, CNRS, IRD, UPS, Toulouse, France
[4] Université Grenoble Alpes, Inria, CNRS, Grenoble INP, LJK, 38000 Grenoble, France
[5] Collecte Localisation Satellites (CLS), Toulouse, France

Corresponding author: Kenza Himmich (kenza.himmich@locean.ipsl.fr)

Key Points:

- The Antarctic sea ice season duration has undergone an unprecedented shortening since 2016;
- The changes include thinner ice, faster melt, earlier retreat, larger ocean heat uptake, later advance, in line with the ice-albedo feedback;
- The near-circumpolar ice thinning is consistent with a possible increase in sensible heat supply by the ocean.

Abstract

Antarctic sea ice extent has been persistently low since late 2016, possibly owing to changes in atmospheric and oceanic conditions. However, the relative contributions of the ocean, the atmosphere and the underlying mechanisms by which they have affected sea ice remain uncertain. To investigate possible causes for this sea-ice decrease, we establish a seasonal timeline of sea ice changes following 2016, using remote sensing observations. Anomalies in the timing of sea ice retreat and advance are examined along with their spatial and interannual relations with various indicators of seasonal sea ice and oceanic changes. They include anomalies in winter ice thickness, spring ice removal rate due to ice melt and transport, and summer sea surface temperature. We find that the ice season has shortened at unprecedented rate and magnitude, due to earlier retreat and later advance. We attribute this shortening to a winter ice thinning, in line with the ice-albedo feedback, with ice transport playing a more minor role. Reduced ice thickness has accelerated spring ice area removal as thinner sea ice requires less time to melt. The consequent earlier sea ice retreat has in turn increased ocean solar heat uptake in summer, ultimately delaying sea ice advance. We speculate that the observed winter sea ice thinning is consistent with previous evidence of subsurface warming of the Southern Ocean.

Plain Language Summary

Following 2016, the Antarctic sea ice cover has been persistently low. To understand why, we retrace the seasonal timeline of sea ice and oceanic changes, using satellite observations. We find that the sea ice season has been significantly shorter following 2016, due to a later start and an earlier end. This shortening is likely caused by thinner sea ice in winter, accelerating sea ice melt in spring and causing sea ice to disappear earlier. In turn, this has caused the ice-free ocean to absorb more solar heat in summer, and take longer to cool down in the fall, ultimately delaying the ice season onset. Warmer waters beneath the Southern Ocean's surface, as evidenced by previous studies, could be a plausible cause of the observed winter sea ice thinning.

1 Introduction

Antarctic sea ice has been subject to puzzling changes since the start of remote sensing observations. Over more than three decades, there was a striking contrast between the substantial decrease in Arctic sea ice (Cavalieri & Parkinson, 2012) and the overall weak but clear increase in Antarctic sea ice (Comiso, 2017; Parkinson & Cavalieri, 2012). In late 2016, however, Antarctic sea ice extent underwent an abrupt decline, sustained in the following years by several record lows (Parkinson, 2019; Raphael & Handcock, 2022).

The initial decrease in late 2016 has been mainly attributed to atmospheric processes. Anomalous winds produced by tropical teleconnections (Meehl et al., 2019) and a negative phase of the Southern Annular Mode (SAM; Schlosser et al., 2018; Turner et al., 2017) have warmed the surface ocean (Meehl et al., 2019) and limited the northward expansion of sea ice (Stuecker et al., 2017; Turner et al., 2017). By contrast, the sustained low sea ice state following 2016 has been attributed to both oceanic and atmospheric changes. Atmospheric changes include strengthened southward winds (Schroeter et al., 2023) and increased storm frequency (Turner et al., 2022). However, simulations using a coupled climate model suggest that the sole contribution of the atmosphere is insufficient to explain observed sea ice changes (Zhang et al., 2022). Instead, several studies point to a warming of the Southern Ocean subsurface as a key potential cause of the low sea ice state (Meehl et al., 2019; Purich & Doddridge, 2023; Zhang et

al., 2022). Notably, the post-2016 shift in the seasonal persistence of sea ice anomalies (Purich & Doddridge, 2023), which is linked to the vertical structure of oceanic properties (Holland et al., 2013; Libera et al., 2022), suggests that recent subsurface ocean and sea ice changes could be connected. Subsurface warming has been identified as a long-term response to a phase of negative Interdecadal Pacific Oscillation (IPO) and positive SAM, with resulting Ekman suction of warm subsurface waters (Ferreira et al., 2015; Kostov et al., 2017; Meehl et al., 2016). Northward sea ice transport induced by a positive SAM may have also contributed to this warming by increasing stratification and reducing subsurface ventilation (Haumann et al., 2020). Yet, how changes in atmospheric and oceanic conditions have affected sea ice remain unclear. Moreover, further evidence is required to establish the predominant role of subsurface warming over atmospheric processes in driving the recent sea ice changes.

Next to ice extent, useful markers of sea ice changes include the dates of advance and retreat, which represent two key transitions in the seasonal cycle of sea ice. Sea ice advance or retreat dates respectively mark the start and end of the sea ice season, defined as the first day in the year when sea ice concentration exceeds or falls below 15% (Massom et al., 2008; Stammerjohn et al., 2008). These two metrics allow for spatial analysis across the entire seasonal ice zone, and highlight which regions are changing, and which are not.

Changes in the timing of sea ice retreat and advance can be respectively traced back to prior ice thickness (Smith et al., 2020) and mixed layer heat content (Himmich et al., 2023). On the grid-point scale, a reduction in ice thickness implies a larger prevalence of thin ice that is removed more efficiently upon melting (Holland et al., 2006), and thus retreats earlier. Thinner ice promotes solar radiation uptake, basal melting (Maykut & McPhee, 1995; Maykut & Perovich, 1987; Vivier et al., 2016) and accelerates sea ice concentration decreases. Also, earlier retreat increases solar radiation uptake (Perovich et al., 2007) and the mixed layer heat content during the open water season, delaying sea ice advance (Himmich et al., 2023; Holland et al., 2017; Stammerjohn et al., 2012). Both processes are linked to ice-albedo feedbacks. Ice transport also contributes to changes in sea ice seasonality by modifying sea ice concentration (Holland et al., 2017; Holland & Kwok, 2012) or, more indirectly, by increasing the open water fraction and triggering the ice-albedo feedback (Holland et al., 2017; Massom et al., 2008; Stammerjohn et al., 2008). Examining changes in sea ice seasonality alongside changes in ice thickness, ocean heat content and ice concentration budget can therefore provide valuable insights into the drivers of the sea ice shift following 2016. However, changes in sea ice seasonality have only been documented until 2012, with large regional trends towards later retreat and earlier advance in the Amundsen and Bellingshausen Seas and, earlier retreat and later advance in the Ross Sea (e.g. Simpkins et al., 2013). Possible shifts in sea ice seasonality following 2016 have yet to be investigated.

In this study, we evaluate the changes in sea ice seasonality following 2016, based on passive microwave sea ice concentration records. We analyze possible drivers of these changes using satellite observations sea ice of thickness, sea surface temperature and ice concentration budget diagnostics, including ice-albedo feedback processes and ice transport. Finally, we discuss whether those changes point to the atmosphere or the ocean as the key driver of the recent sea-ice shift.

2 Materials and Methods

2.1 Sea ice concentration budget

To unravel the thermodynamic and dynamic nature of the processes contributing to the recent sea ice changes, we use a sea ice concentration budget decomposition based on the governing equation for sea ice concentration (C; Holland & Kwok, 2012):

$$\frac{\partial C}{\partial t} = -\nabla.(uC) + residual \quad (1)$$

$$\nabla.(uC) = u.\nabla C + C\nabla.u \quad (2)$$

where u is the sea ice drift field. The dynamic term ($\nabla.(uC)$) represents advection ($u.\nabla C$) and divergence ($C\nabla.u$) of sea ice caused by ice drift whereas the residual term includes both thermodynamic processes (melting / freezing) and mechanical redistribution (ridging/rafting).

We apply the exact methodology of Holland & Kimura (2016) on OSI SAF sea ice concentration and drift data to compute the dynamic and residual contributions to the budget. Sea ice concentration fields are interpolated on the 75-km grid of ice drift. A 7x7 cell square-window smoothing filter is then applied to the ice drift fields in order to avoid noise in the dynamic term. The time derivative in ice concentration is calculated as a central difference in time of sea ice concentration fields at a daily frequency. Advection and divergence terms are calculated as central differences in space then averaged over 3-days periods to synchronize with time derivatives.

2.2 Diagnostics of sea ice and sea surface changes

In this study, we consider that each year starts and ends in September, during the ice season. For example, 1980 starts on September 15th 1979 and ends in September 14th 1980.

To diagnose the changes in sea ice seasonality, we derived the dates of sea ice retreat and advance from the EUMETSAT Ocean and Sea Ice Satellite Application Facility (OSI-SAF) sea ice concentration, on which we applied a 15-day temporal filter to avoid retaining any date reflecting short events (Lebrun et al., 2019). The date of retreat is defined as the first day filtered sea ice concentration drops below 15% while the date of advance is the first day filtered sea ice concentration exceeds 15%, similar to previous studies (Lebrun et al., 2019; Parkinson, 1994; Simpkins et al., 2013; Stammerjohn et al., 2012). To ensure retreat dates and subsequent advance dates of the same yearly seasonal cycle are retained, we looked for advance (retreat) dates starting on a month where no sea ice advance (retreat) occurs, on average over 1980-2022. We selected January 1st of the current year as the start date for advance, and May 1st of the previous year for retreat, since most of advance and retreat dates occurs after those dates. Ultimately, for each year, only the dates between September 15th of the previous year and September 14th of the current year are retained.

To diagnose possible changes during the ice and open water seasons, we respectively use mean September sea ice thickness, representing the end-of-winter thickness, and seasonal maxima of sea surface temperature. Each yearly sea surface temperature maximum was selected between the retreat date and the following advance date of the corresponding year.

To investigate the changes in spring ice removal processes possibly leading to changes in the retreat dates, we define the spring (over October, November and December) sea ice removal rate (IRR) as:

$$IRR = -\int_{OND} \frac{\partial C}{\partial t}_{<0} \, dt \quad (3)$$

The IRR filters the positive derivatives to ensure focus on removal processes. Using the sea ice concentration budget decomposition, we also calculate the dynamic and residual contributions to the IRR for each year over 1992-2020. Climatological fields of IRR and contributions show that the dynamic term is positive in the inner sea ice zone due to ice export out of that inner zone and negative in the outer sea ice zone due to ice import into that outer zone (see Supplementary Figure 1). This dynamic contribution is, however, small compared to the residual, which dominates the removal rate over all the seasonal ice zone. Based on these considerations, positive (negative) anomalies in IRR can be interpreted as an increase (decrease) in ice removal. Positive (negative) anomalies in dynamic contribution would suggest increased (decreased) ice export in the inner pack and decreased (increased) ice import in the outer pack. Interpreting the sign of anomalies in residuals is not as straightforward because it accounts for both melt and mechanical redistribution processes.

For any statistical calculations conducted in this study involving the previously mentioned diagnostics, a missing value is assigned where the number of years with undefined retreat or advance dates (corresponding to year-round ice-free or ice-covered grid points) is less than one third of the total number of years in the considered period, following Lebrun et al., 2019. This procedure ensures that meaningful and consistent averages, trends or correlations are obtained.

3 Data

This study is based on satellite observations of sea ice concentration, drift, thickness and sea surface temperature. We use daily passive microwave sea ice concentration over 1979-2022 (Lavergne et al., 2019) and sea ice drift over 1991-2020 (Lavergne & Down, 2023) from OSI-SAF, with respective resolutions of 25 and 75 km. Fields of sea ice drift are retrieved using different methods according to the season. In winter, from April to September, ice drift is retrieved using a maximum cross correlation algorithm applied to brightness temperature from a number of sensors (SSM/I, SSMIS, AMSR-E and AMSR2). In summer, from November to February, a free-drift model based on the ERA5 wind fields is used (Hersbach et al., 2020). In October and March, the fields are derived from both model and satellite-based outputs.

For sea ice thickness, we utilized altimetry-based ice thickness retrievals from 1994 to 2022, as provided by (Bocquet, 2023; Bocquet & Fleury, 2024). This dataset integrates year-round 12.5 km gridded radar freeboard time series from ERS-1, ERS-2, Envisat, and CryoSat-2 missions. Different missions are inter-calibrated, leveraging mission overlap. Ku-band radar echoes are corrected for the varying speed of light in snow (Mallett et al., 2020) and converted to radar freeboards following the methodology outlined by Laxon et al. (2003). The density of ice (875-920 kg/m^3) and snow (320-350 kg/m^3) includes specified seasonal variations (Kurtz & Markus, 2012; Maksym & Markus, 2008). Snow depth is taken from a climatology of radiometer-based estimation developed for SI-CCI (Paul, S. et al., 2021). Finally the ice thickness is deduced from the radar freeboard and the snow using the equilibrium equation of the

snow covered ice in the sea water. The resulting ice thickness dataset was evaluated against the ASPeCt dataset (Worby, Geiger, Paget, Woert, et al., 2008), AWI moorings in the Weddell Sea (Behrendt et al., 2013), and Operation Ice Bridge (Kurtz et al., 2013), resulting in reasonable agreement despite potential biases.

Finally, we use a daily satellite product of sea surface temperature available over 1982-2022, based on thermal infra-red radiance measurements, and taken from the global L4 (gap-free, gridded) European Space Agency (ESA) SST Climate Change Initiative (CCI) analysis with a resolution of 0.05° (Merchant et al., 2019).

All data are either interpolated on the OSI-SAF Equal-Area Scalable Earth 2 (EASE2) 25 km or 75 km grid.

4 Unprecedented shortening of the sea ice season following 2016

We examine the changes in ice season duration and ice retreat and advance date over 1980-2022 (Figure 1), based on mean anomalies over the seasonal ice zone (see Figure 2).

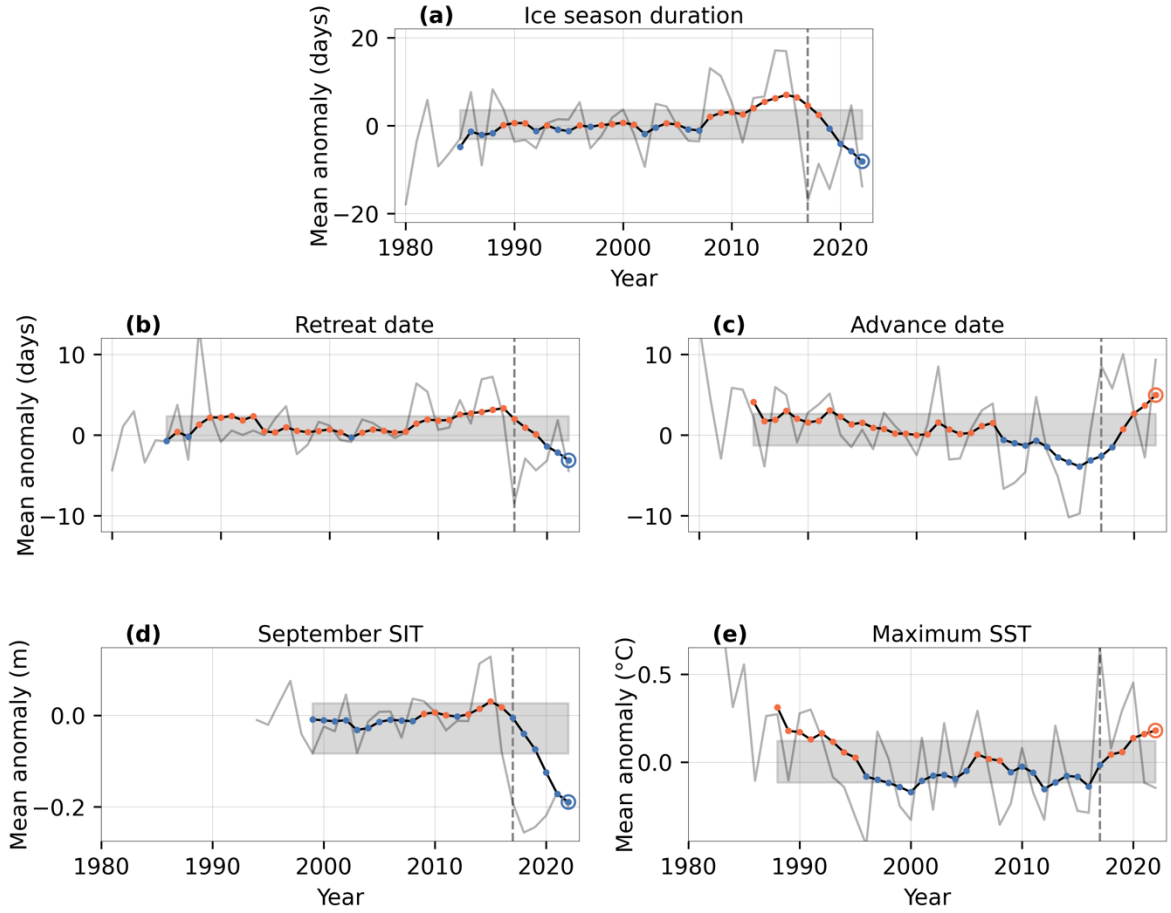

Figure 1. Time series of selected sea ice and ocean diagnostics. Grey solid lines show yearly anomalies averaged over the seasonal ice zone in **a**, ice season duration, **b**, retreat dates, **c**, advance dates, in **d**, September sea ice thickness (SIT) and **e**, maximum sea surface temperature (SST). Black lines with colored dots show 6-year moving averages such that the last point represents the 2017-2022 mean anomalies depicted in Figure 2. Anomalies are relative to 1980-

2016 in **a**, **b** and **c**, to 1983-2016 in **d** and to 1994-2016 in **e**. Red dots mark positive values whereas blue dots mark negative values. Stippled grey lines mark the 2017 yearly anomalies. The grey areas delimit the mean +/- the standard deviation of 6-year moving averages over the whole time series.

Over 1980-2016, the sea ice season duration exhibits a clear increase of 3.6 days per decade (Figure 1a; Table 1) due to trends towards 1 day later retreat and 2.6 days earlier advance per decade (Figures 1b and c). Over 2016-2017, however, an abrupt shortening occurs, followed by large negative anomalies maintaining the ice season duration at low values until 2022 (Figures 1a-c). As a result of this reversal in behavior after 2016, the ice duration trend over 1980-2022 is small and not statistically significant (Table 1). The weakening of circumpolar trends results from regional pattern changes, evident when comparing regional trends over 1980-2022 and 1980-2016 (see Supplementary Figure 2). The largest regional trends towards a longer ice season prior to 2017, located in the Ross and Weddell Seas, have weakened over 1980-2022. Additionally, significant trends towards a shorter ice season have emerged in the Bellingshausen Sea and the Indian sector over 1980-2022. Spatial patterns of ice season length anomalies following 2016 align consistently with the evolution of regional trends (Figures 2a-c). Based on the 6-year averaged anomalies over 2017-2022, we find that the ice season shortening is overall circumpolar, but largest in the Ross, Bellingshausen, Weddell and Indian sectors. On average over the seasonal ice zone, the ice season is 8.9 days shorter in 2017-2022 compared to 1980-2016, due to 3.7 days earlier retreat and 5.2 days later advance.

Table 1. Long-term trends in selected sea ice and ocean diagnostics. Trends are defined as the linear least square fit slopes for the yearly anomalies, averaged over the seasonal ice zone, over time periods ending either in 2016 or in 2022. Time periods are chosen according to underlying data availability and are indicated in the first column of the table. Slopes standard errors are given as uncertainties. Bold numbers indicate statistically significant trends at the 95% level.

	Trends ending in 2016	Trends ending in 2022
Ice season duration (days/dec.) 1980-2022	**3.6 +/- 1.0**	0.6 +/- 1.0
Retreat date (days/dec.) 1980-2022	**1.0 +/- 0.5**	-0.2 +/- 0.5
Advance date (days/dec.) 1980-2022	**-2.6 +/- 0.6**	-0.8 +/- 0.6
September SIT (cm/dec.) 1994-2022	1.8 +/- 1.8	**-6.0 +/- 2.0**
Maximum SST (°C/dec.)	**-0.15 +/- 0.04**	-0.06 +/- 0.04

1983-2022

We next assess the magnitude and rate of the recent ice season shortening. We find that the mean anomalies in ice season length, retreat and advance dates for 2017-2022 with respect to 1980-2016 (Figures 1a-c) are larger than any previous 6-year mean anomalies. Specifically, the 2017-2022 anomaly in ice season duration is the lowest on record, being 2 days shorter than the previous shortest ice season anomaly (2016-2021) and exceeding three times the standard deviation (Figures 1a). The 2017-2022 anomaly is also record breaking for both retreat and advance dates by approximately 1 day (Figures 1b, c). This indicates that the earlier retreat, later advance and consequent shorter sea ice season following 2016 are unprecedented. The interannual changes in sea ice seasonality are also unusually rapid when comparing 7-year periods ending after 2017, exceeding the standard deviation in mean rates of change (Figures 3a-c). The fastest 7-year changes in retreat and advance dates over the entire time series occur over the 2013-2019 and 2014-2020 periods, respectively (i.e., ending in 2019 and 2020, as shown in Figures 3b, c), reaching respectively more than 3 times and 2 times the standard deviation.

Due to a near-circumpolar shortening following 2016, the evolution of sea ice season duration over 1980-2022 closely parallels the changes observed in ice extent, with a long-term increase followed by an unprecedentedly large and rapid decrease in 2017, as shown by Parkinson (2019).

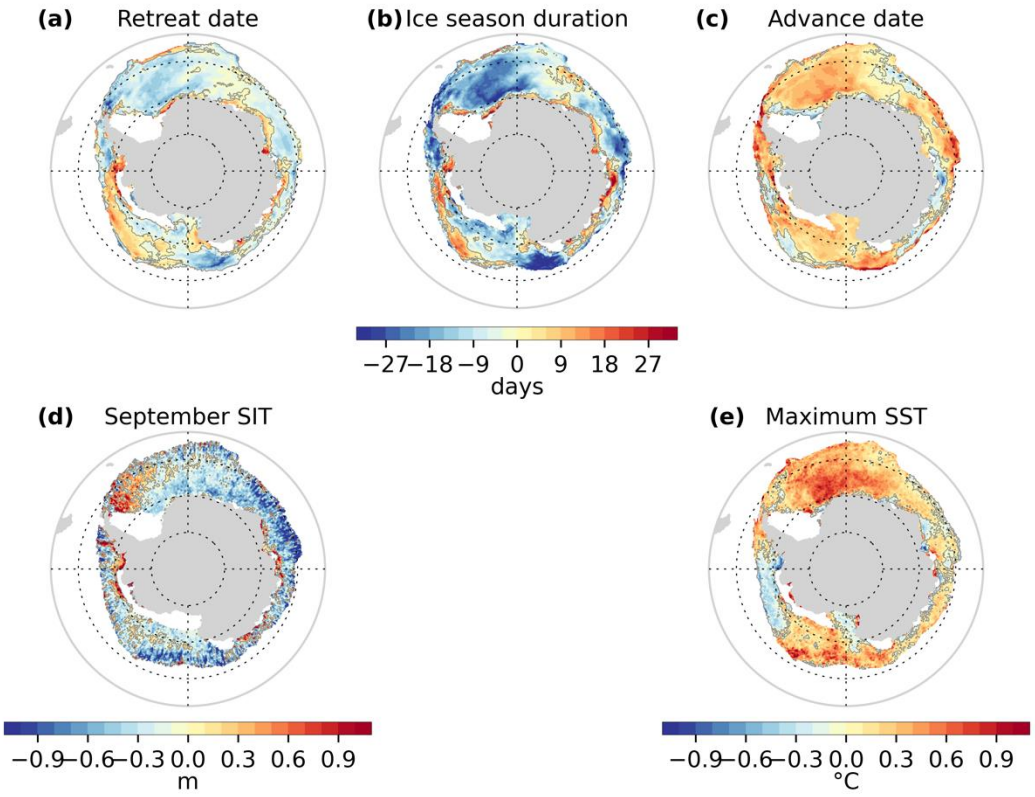

Figure 2. Mean anomalies in selected sea ice and ocean diagnostics over 2017-2022. **a**, Ice season duration, **b**, retreat dates, **c**, advance dates, **d**, September sea ice thickness (SIT), **e**, maximum sea surface temperature (SST). Anomalies are relative to 1980-2016 in **a**, **b** and **c**, to 1983-2016 in **d** and to 1994-2016 in **e**. White patches indicate regions out of the seasonal ice zone.

5 Drivers of the recent sea ice season shortening

5.1 Shorter ice season: response to ice thinning?

We hypothesize that the recent ice season shortening might be tied to changes in ice thickness and upper ocean heat content. Accordingly, in this section, we examine the changes in the September sea ice thickness over 1994-2022 and in the seasonal maximum of sea surface temperature, used as a proxy of the summer mixed layer heat content (Himmich et al., 2023), over 1983-2022.

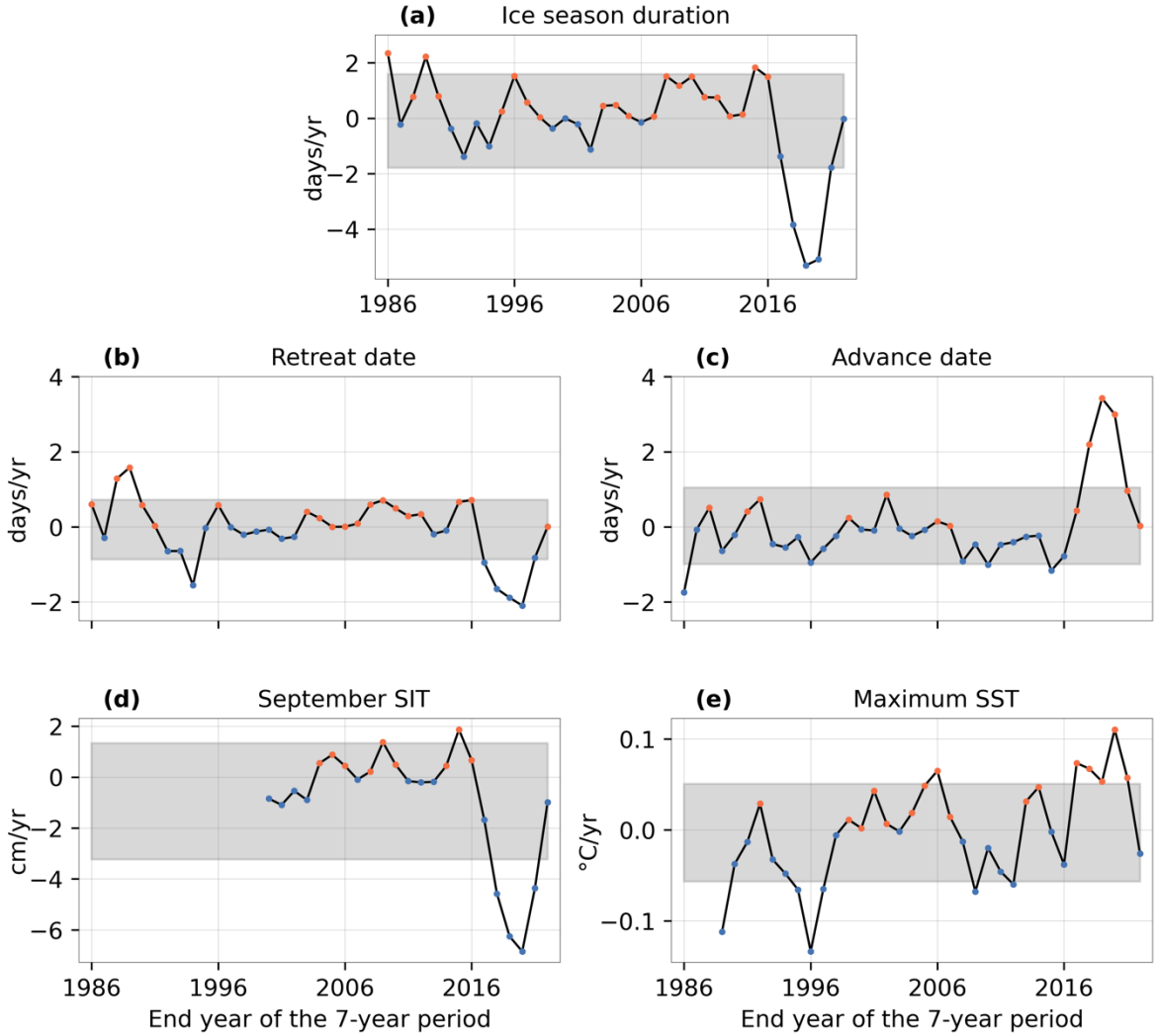

Figure 3. Rate of seven-year changes in selected sea ice and ocean diagnostics. Rates are calculated as least-square slopes over 7 years of mean anomalies over the seasonal ice zone in **a**, Ice season duration, **b**, retreat date, **c**, advance date **d**, September sea ice thickness (SIT), and **e**, maximum of sea surface temperature (SST). Blue dots mark negative values whereas red dots mark positive values. The grey areas delimit the mean +/- the standard deviation over the whole time series.

Similar to retreat and advance dates, September ice thickness and maximum sea surface temperature have undergone an unprecedented shift since 2016. This finding is based on mean anomalies over the seasonal ice zone (Figures 1d, e). Over 1994-2016, sea ice thickness anomalies exhibit no statistically significant trend, while over the 6-year thickness time series ending in 2022, a statistically significant trend emerges, showing at decrease of 6 cm per decade. A shift is also observed for sea surface temperature in 2016. Over 1983-2016, maximum sea surface temperature anomalies exhibit a statistically significant trend toward colder sea surface temperatures by 0.15°C per decade. However, over 1983-2022, the trend becomes almost nil (Table 1). This shift in long-term trends stems from widespread thinner sea ice and warmer sea surface following 2016 (Figure 2d, e), occurring at an unprecedented magnitude and rate. Notably, the average anomaly over 2017-2022 is the lowest on record for thickness and the second highest on record for temperature, among 6-year average anomalies (Figures 1d, e). Moreover, the top 3 7-year periods with fastest sea ice thinning and sea surface warming end after 2017 (Figures 3d, e).

The coinciding earlier retreat, later advance, thinner sea ice and warmer sea surface temperatures suggest that these variables could be linked and driven by a common underlying mechanism. That the post-2016 ice thinning and sea surface warming (Figures 2d, e) occur mainly where the changes in retreat and advance date are the largest (see Supplementary Figure 3) further supports this hypothesis. Remarkably, we find that 74% of seasonal ice zone grid points with earlier retreat spatially correspond to thinner September sea ice. Earlier retreat due to thinning reflects either a thermodynamic response, with increased melt rate, or a dynamic response, with increased sensitivity to transport, as suggested by Holland et al. (2006). This point will be further investigated in the next section. In addition, we find that 85% of the grid points with higher maximum sea surface temperature also show an early retreat. In turn, 92% of grid points with later advance have a higher sea surface temperature. The correspondence between earlier retreat, warmer sea surface temperature and later advance is consistent with ice-albedo feedback processes during the open water season (Himmich et al., 2023; Holland et al., 2017; Stammerjohn et al., 2012): earlier retreat increases solar heat uptake into the mixed layer; the extra heat needs more time to be released, which delays sea ice advance. Accordingly, 77% of the grid points with later sea ice advance also have earlier ice retreat.

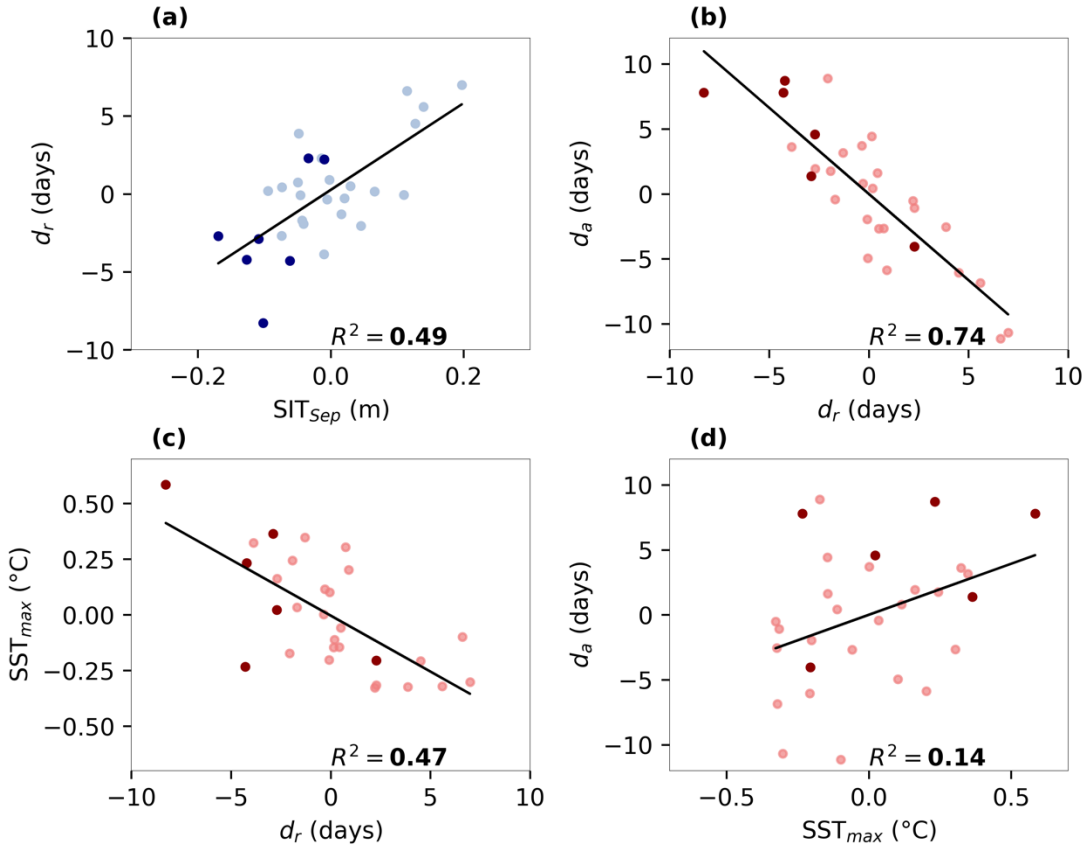

Figure 4. Interannual relationships between selected sea ice and ocean diagnostics, over 1994-2022. Detrended anomalies of **a**, retreat dates (d_r) versus September sea ice thickness (SIT_{Sep}), **b**, advance dates (d_a) versus d_r, **c**, maximum sea surface temperature (SST_{max}) versus d_r, **d**, d_a versus SST_{max}. Blue tones indicate ice season relations whereas red tones indicate open water season season, as illustrated in Figure 5. 2017-2022 anomalies are marked in dark colours. A Least Square linear regression was performed for each plot; the corresponding regression line (significant at 99%), and corresponding coefficients of determination (R^2) are shown. The 1994-2022 period was selected to ensure consistency of the analysis, as all relevant diagnostics are available over this timeframe.

Yearly anomalies follow a consistent sequence of processes: low winter thickness results in early retreat, increased summer ocean heat content, and late advance. For instance, in 2016/17, the anomalously low September sea ice thickness comes first in order, followed by the earlier retreat, warmer maximum sea surface temperature and ultimately, later advance (Figure 1). Correlations between 1994-2022 time series of mean detrended anomalies averaged over the seasonal ice zone support this analysis, with this specific period selected due to the availability of relevant diagnostics. We observe a statistically significant link ($R^2 = 0.49$, $p < 0.01$) between the mean September sea ice thickness and the subsequent mean retreat date (Figure 4a). This relationship indicates that for each centimeter of ice thinning, the retreat occurs 0.28 days earlier. We also observe a statistically significant link between retreat and subsequent advance date anomalies ($R^2 = 0.74$, $p < 0.01$), indicating a delay in advance of 1.3 day per day of early retreat

(Figure 4b). The link between anomalies in retreat date and subsequent maximum sea surface temperature appears relatively strong ($R^2 = 0.47$, $p < 0.01$; Figure 4c), when compared with the link between maximum sea surface temperature and subsequent advance date ($R^2 = 0.14$, $p < 0.01$; Figure 4d). We argue this reflects the importance of accounting for mixed layer depth to accurately evaluate the mixed layer heat content when the ocean is cooling down during open water season (Himmich et al., 2023). The maximum sea surface temperature is potentially a better proxy of the mixed layer heat content during the warming period, due to shallower mixed layers, explaining why the temperature is more strongly linked to retreat dates than to advance dates.

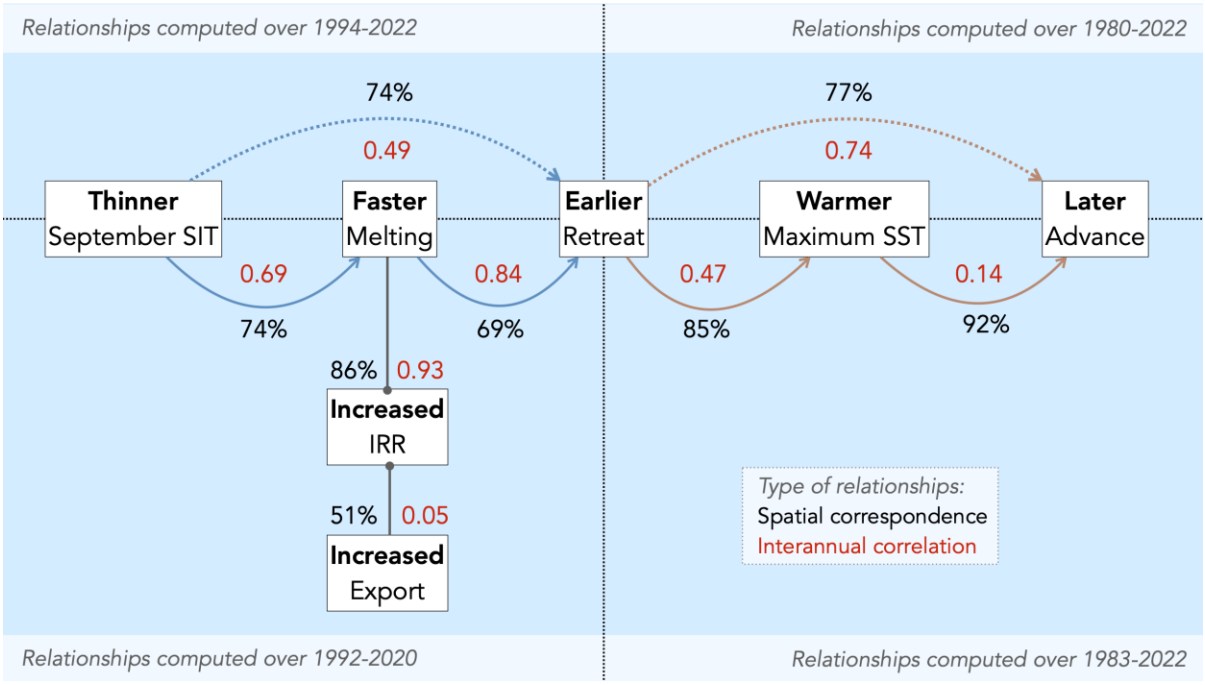

Figure 5. Schematic of the thermodynamic response of sea ice and sea surface to the ice thickness reduction following 2016. Colored lines represent ice-albedo feedback processes occurring within the sea-ice season (blue) versus open water season (red), processes that link winter sea ice thickness (SIT) to spring ice removal rate (IRR) and retreat date, to summer seasonal maximum of sea surface temperature (SST) and subsequent autumn advance date. Grey lines represent the dynamic and thermodynamic contributions to the IRR. Red numbers refer to the coefficient of determination of interannual correlations between the considered variables, as shown in Figures 4 and 7. Percentages quantify the spatial correspondence between specified variable changes following 2016, based on mean anomalies (see Figures 2, 6 and Supplementary Figure 3). The time period considered for each spatial relationship, which depends on underlying data availability, is specified on the schematic.

Based on these spatial and interannual linkages (see Figure 5), we surmise that the decrease in the September ice thickness has contributed to the earlier sea ice retreat following 2016. This has, in turn, lead to a warming of the upper ocean and delayed sea ice advance through the ice-ocean feedback. However, whether the ice thinning is a result of thermodynamic or dynamic changes remains to be established.

348

349 5.2 Earlier retreat: a dynamic or thermodynamic response of ice thinning?

350 To unravel the thermodynamic or dynamic nature of the relationship between ice thinning
351 and early retreat, we examine melt season processes based on a sea ice concentration budget
352 derived from passive-microwave concentration and drift. We evaluate the average sea ice area
353 removal rate (IRR) over spring (October, November, December) as well as the dynamic and
354 residual contributions to the IRR, over 1992-2020. The dynamic contribution to the IRR is
355 mostly due to the northward export of sea ice (see Supplementary Figure 1) whereas residuals
356 include both melting and, also, to some extent, mechanical redistribution through ridging and
357 rafting (Holland & Kimura, 2016).

358 We find that the post-2016 shift is also seen in the spring ice removal processes. Mean
359 IRR anomalies decrease to lower than average values over 1992-2016, then undergo an
360 unprecedentedly rapid rise (see Supplementary Figure 4) starting in the spring before the early
361 ice retreat of 2017 (Figure 6a). Anomalies in the residual contribution to the IRR evolve
362 similarly (Figure 6c) and account for 93% of the interannual variance in total IRR (Figure 7a).
363 Conversely, anomalies in the dynamic contribution show comparatively small variations (Figure
364 6e) and only explain 5% of the variance in total IRR (Figure 7b).

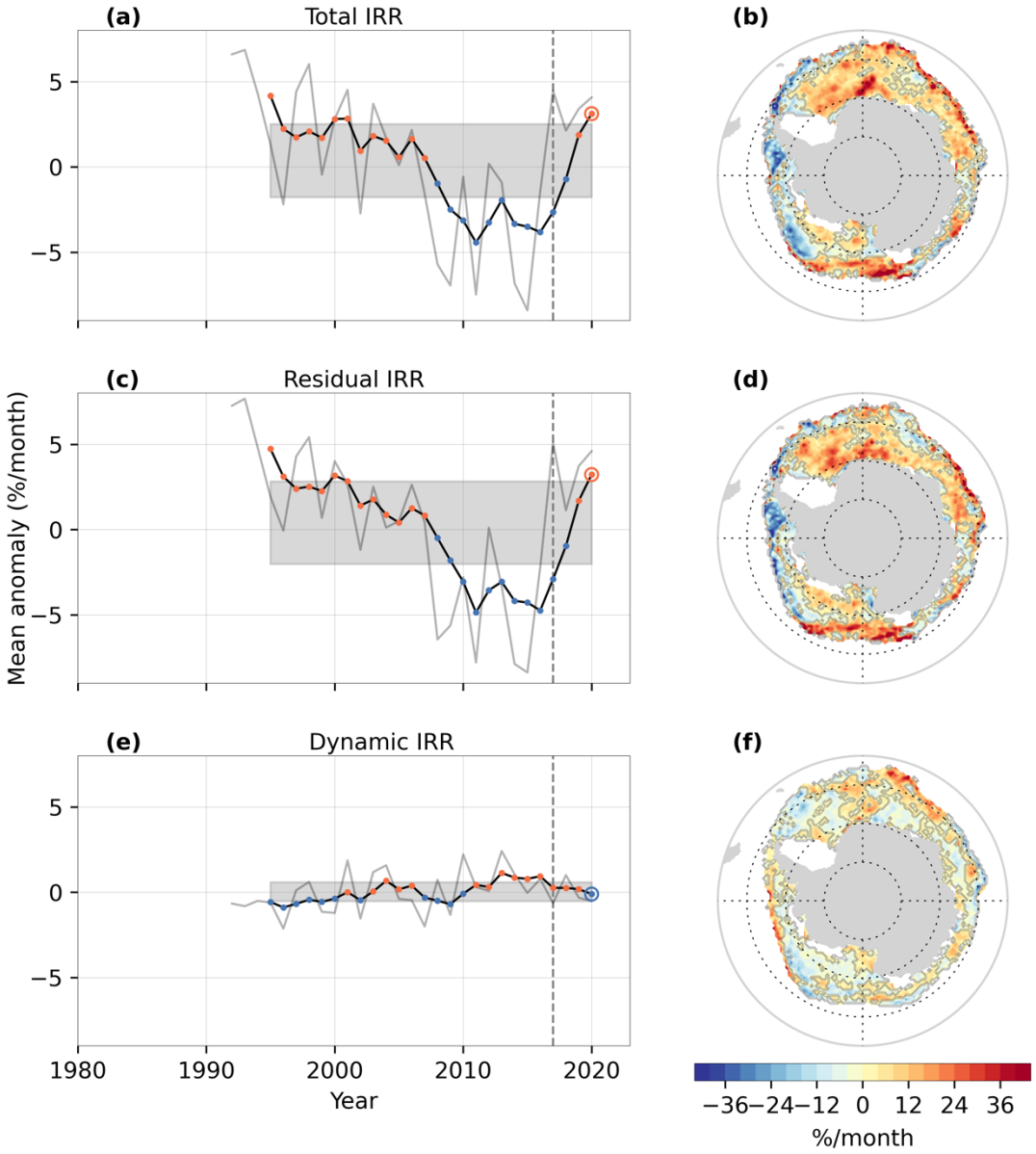

Figure 6. Changes in the spring sea ice removal rate (IRR) and its contributions over 1992-2020. Grey solid lines show yearly anomalies averaged over the seasonal ice zone in **a**, total IRR, **c**, residual IRR, **e**, dynamic IRR (grey lines). Black lines in **a**, **c** and **e** show 4-year moving averages such that the last point represent the 2017-2020 mean anomalies depicted in **b**, for total IRR, **d**, for residual IRR and **f**, for dynamic IRR. Anomalies are relative to the 1992-2016 average. Red dots mark positive values whereas blue dots mark negative values. Stippled grey lines mark the 2017 yearly anomalies. The grey areas delimit the mean +/- the standard deviation of 4-year moving averages over the whole time series.

Residuals thus appear to be the major contributor to the recent increase in IRR compared to sea ice export. This is also highlighted by similar spatial patterns of mean anomalies over 2017-2020 in IRR and residual contribution (Figure 6b and d). Notably, 86% of the seasonal ice zone grid points with increased IRR correspond to increased residual contribution. By contrast, substantial discrepancies are observed between the spatial mean anomalies of the IRR and of the

dynamic contribution (Figure 6b and f). Furthermore, the absence of ice thickening in spring (see Supplementary Figure 5) in regions of increased residual contribution (Figure 6d) suggests that ridging and rafting weakly contribute to the IRR, and that thermodynamics must dominate the increase. Hence, the recent IRR increase is likely caused by a more rapid melt-back.

We next investigate how the recent changes in residual IRR would relate to changes in September sea ice thickness and retreat date. We find that 74% of grid points showing an increase in residual IRR (Figure 6d) correspond to thinner sea ice (Figure 2d). Additionally, 69% of grid points with early retreat (Supplementary Figure 3) correspond to increased residual contribution (Figure 6d). The same links are also evident at interannual time scales. Mean detrended anomalies in September sea ice thickness over the seasonal ice zone sectors explain 69% of the interannual variance in residual IRR in the following spring (Figure 7c). In turn, mean detrended anomalies in residual IRR explain 84% of the variance in the following retreat dates (Figure 7d). Spatial and interannual linkages between thinner sea ice, increased residual IRR due to sea ice melt and earlier retreat (see Figure 5) are therefore compatible with a thermodynamic response to sea ice thinning (Holland et al., 2006). Idealized simulations of the sea ice melt period shown in Appendix A feature similar links and highlight that the ice-albedo feedback processes contribute to such response.

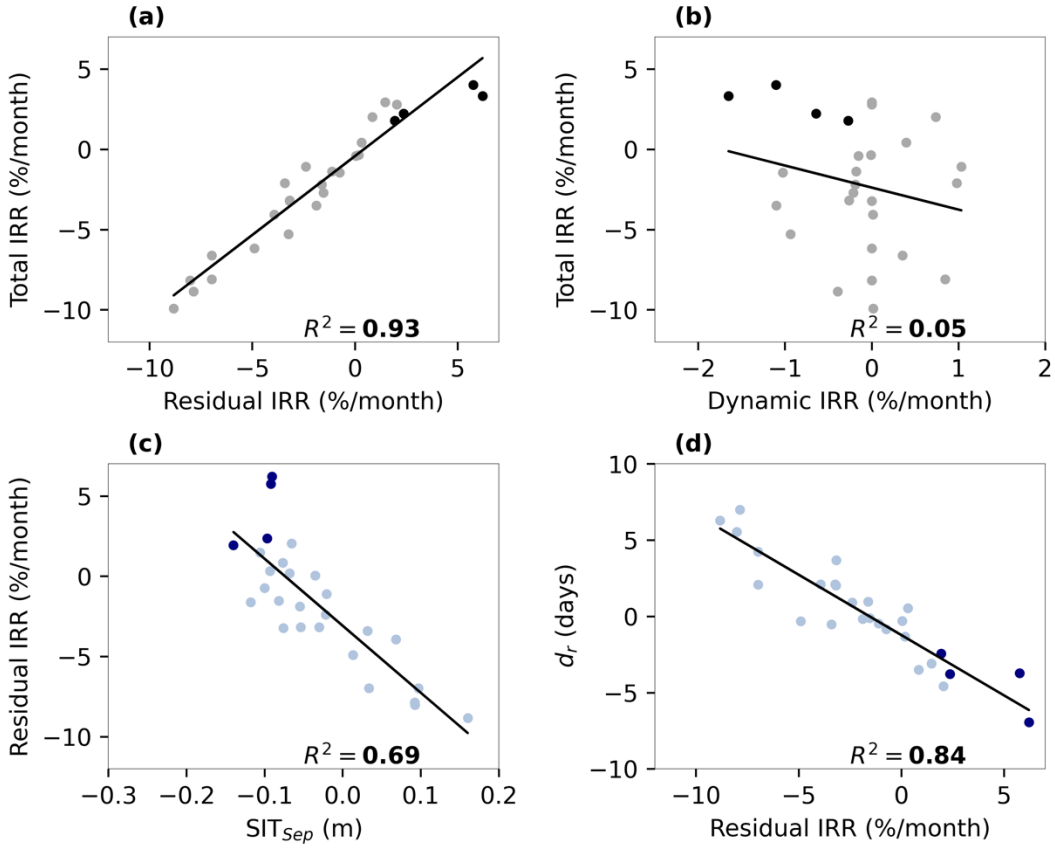

Figure 7. Interannual relationships between the spring sea ice removal rate (IRR) and relevant sea ice diagnostics, over 1992-2020. Detrended anomalies of **a**, total ice removal rate (IRR) versus residual IRR, **b**, total IRR versus dynamic IRR, **c**, residual IRR versus September

sea ice thickness (SIT_{Sep}) **d**, retreat dates (d_r) versus residual IRR. The 2017-2020 anomalies are marked in dark colors. A Least Square linear regression was performed for each plot; the corresponding regression line (significant at 99%), and corresponding determination coefficient (R^2) are shown. The 1992-2020 period was selected to ensure consistency of the analysis, as all relevant diagnostics are available over this timeframe.

6 Discussion and Conclusion

The sea ice season duration has undergone an unprecedented shortening since 2016 due to earlier ice retreat and later advance. These anomalies in the timing of sea ice retreat and advance are strongly linked to anomalies in winter sea ice thickness, summer sea surface temperature and spring ice removal rate related to sea ice melt (Figure 5). The correspondence between thickness and other markers of sea ice and sea surface changes is particularly remarkable considering the large uncertainties associated with satellite observations of sea ice thickness (Kurtz & Markus, 2012). Our findings indicate that the ice season shortening following 2016 is consistent with an ice thinning and the seasonal progression of thermodynamic processes inherent to the ice-albedo feedback (in the sense of Holland et al., 2006), in response to an initial ice thinning. According to our analysis, sea ice transport plays a comparatively minor role, consistently with previous studies highlighting that sea ice changes are primarily driven by thermodynamics (Guo et al., 2023; Kimura et al., 2023).

However, some local exceptions are also visible, where ice-albedo feedback processes do not explain the changes in sea ice seasonality following 2016. First, in the northwest Weddell Sea off the eastern of the Antarctic Peninsula, we find that the mostly earlier retreat (Figure 2b) spatially corresponds to thicker sea ice (Figure 2d) and decreased ice removal rate (Figure 6b). In this region, winter sea ice is thicker but less concentrated, possibly due to increased sea ice divergence (see Supplementary Figure 5). We therefore hypothesize that during spring, the thicker ice might get removed more slowly, and still retreat earlier due to the lower concentration at the start of the melt season. Another possible cause is that there would be a regional high bias in the satellite ice thickness retrieval. Indeed, model and altimetry-based thickness retrievals are particularly inconsistent in that region (Liao et al., 2022). Additionally, in situ sources (Worby, Geiger, Paget, Van Woert, et al., 2008), albeit sparse, do not feature a thickness maximum there.

Second, in the Amundsen Sea and in portions of the eastern Ross Sea and along the East Antarctic coastal regions, a lengthening of the sea ice season is observed (Figures 1b, c). In the Amundsen and eastern Ross Seas, this lengthening mainly corresponds to a later retreat, possibly driven by southerly wind anomalies pushing sea ice (Schroeter et al., 2023) or by increased thickness (Figure 2d), but not necessarily to an earlier advance. There, changes are more likely to be driven by sea ice advection than by thermodynamic processes, as suggested by Kimura et al. (2023), which might explain this spatial mismatch. Off East Antarctica, landfast ice and polynya dynamics may contribute to the sea ice season lengthening. Therefore, for some specific regions, sea ice transport might dominate over ice-albedo feedback processes in driving the changes in sea ice seasonality following 2016.

We next discuss potential atmospheric and oceanic changes contributing to the reduction in sea ice thickness. Enhanced southward winds as evidenced by previous studies (e.g. Nihashi & Ohshima, 2015) could increase ice divergence, thereby favoring the presence of thin newly formed ice. However, in regions of thinner sea ice (Figure 2c), the apparent increase in winter import of ice area suggests otherwise (see Supplementary 5). It is therefore more likely that the

reduced ice thickness results from less growth, which can be due to changes in heat exchanges with the atmosphere and the ocean. Intensified northerly winds may increase warm air intrusions over the Southern Ocean (Schlosser et al., 2018), potentially altering the conductive flux through sea ice and reducing growth. However, increased intrusions of warm air would involve the action of several modes of atmospheric variability (e.g. Clem & Fogt, 2015), which would result in regional reductions in ice thickness rather than in the observed almost circumpolar thinning. By contrast, a near-circumpolar warming of the subsurface ocean, as documented by several studies (Meehl et al., 2019; Purich & Doddridge, 2023; Zhang et al., 2022), could produce the observed reduction in ice thickness.

Warmer subsurface waters could potentially be entrained into the surface layer during winter, when the mixed layer reaches sufficient depth, limiting sea ice growth (Gordon, 1981; Martinson & Iannuzzi, 1998; Saenz et al., 2023; Wilson et al., 2019). Hence, a warmer subsurface ocean serves as a plausible driver of the observed reduction in sea ice thickness, more so than atmospheric changes. Nonetheless, ice-atmosphere feedbacks might amplify the effect of an ocean heat input. Thinner winter sea ice has a lower insulating power, enabling the warm underlying ocean to increase the surface air temperature, in turn leading to further sea ice thinning (Burt et al., 2016).

The cause for the subsurface warming, likely initiated around 2011(Meehl et al., 2019; Purich & Doddridge, 2023), reaching the surface only after 2016 remains unclear. Models suggest that the persistently warm subsurface may have destabilized the mixed layer, inducing the entrainment of these warm waters into the surface (Zhang et al., 2022). However, observational evidence of this destabilization is still lacking. Ultimately, mapping hydrographic changes in the seasonal ice zone, which is beyond the scope of this work, would be required to evaluate the spatial extent of this subsurface warming and better constrain the role of the ocean in driving the recent changes in Antarctic sea ice.

Appendix A: Are the links between observations during the melt period consistent with theory?

What do the links between observed maximum thickness, removal rate and retreat date tell us about the underlying processes? Are they consistent with what we know of the Antarctic sea ice melting process?

To address this, we performed idealized model simulations of the spring sea ice decay and diagnose the same relationships as from observations. Our model encapsulates physics of sea ice melting in the Antarctic, in particular the effect of the ice-albedo feedback (IAF) on basal melting. The IAF is here viewed in the sense of Holland et al. (2006) and describes how solar radiation uptake amplifies a small change in ice concentration by promoting basal melt of thin ice, further reducing ice coverage.

A.1 Model description

We consider a given ice-covered region of the ocean (e.g., a satellite pixel), characterized by ice concentration $A(t)$ and mean thickness $h(t)$, and a surface ocean layer of constant thickness $h_w = 20$ m (Figure A1). External heat inputs to the surface ocean-sea ice system are net solar radiation uptake and sensible ocean heat flux. The surface ocean layer temperature is fixed at the freezing point, so that any heat absorbed in the surface layer is converted into basal melt.

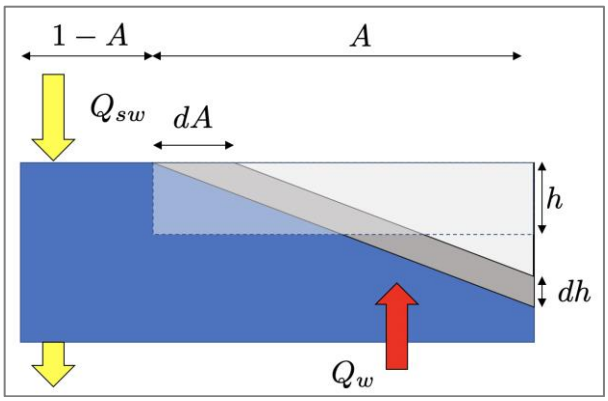

Figure A1. Schematic view of the melting process as viewed in the model.

Net solar radiation uptake in the ocean surface layer (W/m^2) results from the balance of incident, absorbed and transmitted solar radiation, assuming absorption of most solar radiation in a thin surface layer and exponential attenuation with depth (Lengaigne et al., 2007):

$$Q_{sw} = Q_{sw}^{\downarrow}(1-\alpha_w)\cdot[1-(1-R)\cdot\exp(-\kappa h_w)]. \quad \text{(A. 1)}$$

$Q_{sw}^{\downarrow}$ is the incident solar radiation (W/m^2), $\alpha_w = 0.06$ is the ocean albedo, $R = 0.58$ is the fraction of solar radiation absorbed in a small (~10 cm) surface layer and κ = 1/23 m^{-1} is the bulk solar attenuation coefficient.

Ice thickness h decreases due to a prescribed sensible heat flux Q_w and net solar radiation uptake in the surface layer:

$$-\rho L\cdot\frac{dh}{dt} = Q_w + p_1.Q_{sw}\cdot\left(\frac{1-A}{A}\right), \quad \text{(A. 2)}$$

where ρ = 917 kg/m^3 is the ice density and $L = 335000$ J/kg is the latent heat of fusion. The $(1-A)/A$ factor reflects heat conservation: solar radiation penetrates through the open water fraction $(1-A)$ and is attributed over the ice-covered fraction A of the grid cell.

The ice concentration loss rate depends on the subgrid scale ice thickness distribution, and is in particular controlled by the melt rate of thin ice (Holland et al., 2006). Here we assume that the ice thickness is homogeneously distributed between zero and twice the mean. In this context, a decrease in mean thickness implies a loss of thin ice, and the ice concentration decreases as follows:

$$\frac{dA}{dt} = p_2\cdot\frac{A}{2h}\cdot\frac{dh}{dt}. \quad \text{(A. 3)}$$

We also introduce two parameters p_1 and p_2 ([0,1]) that tune solar radiation uptake and the loss of concentration per unit ice thickness.

This approach was introduced in large-scale sea ice models by (Fichefet & Morales Maqueda, 1997; Häkkinen & Mellor, 1990) and is known to provide a sensible first-order emulation of the ice thickness distribution.

A.2 Simulation protocol

We run three ensembles of 150-day sea ice melting simulations, starting with maximum thickness h_{max} and initial ice concentration A_{max} = 0.99. The sensible heat flux Q_w is assumed constant, with a representative value of 30 W/m^2. Solar radiation linearly increases from 50 to

250 W/m^2 from day 1 to day 150, which is representative of the Antarctic sea ice zone from September to December (Vancoppenolle et al., 2011).

We run ensembles of simulations with varying h_{max} from 0.5 to 2.5 m. Three ensembles are run. In the control ensemble, both shortwave enhancement and ice concentration loss are active ($p_1 = p_2 = 1$). They are switched off separately in the two other ensembles.

The simulations feature a rapid ice concentration and thickness loss, and achieve complete ice decay within a few weeks. From each simulation, we diagnose the average removal rate as the mean of *dA/dt* over the whole simulation period, and the retreat date as the last day of simulation with $A > 15\%$.

A.3 A few insights from simulations

Figure A2 shows the simulations outputs. We find that, first, simulated relationship between d_r and h_{max} is linear, whereas the relationship between *IRR* and the two other variables is non-linear. The relationships are not largely responding to sensible oceanic heat flux.

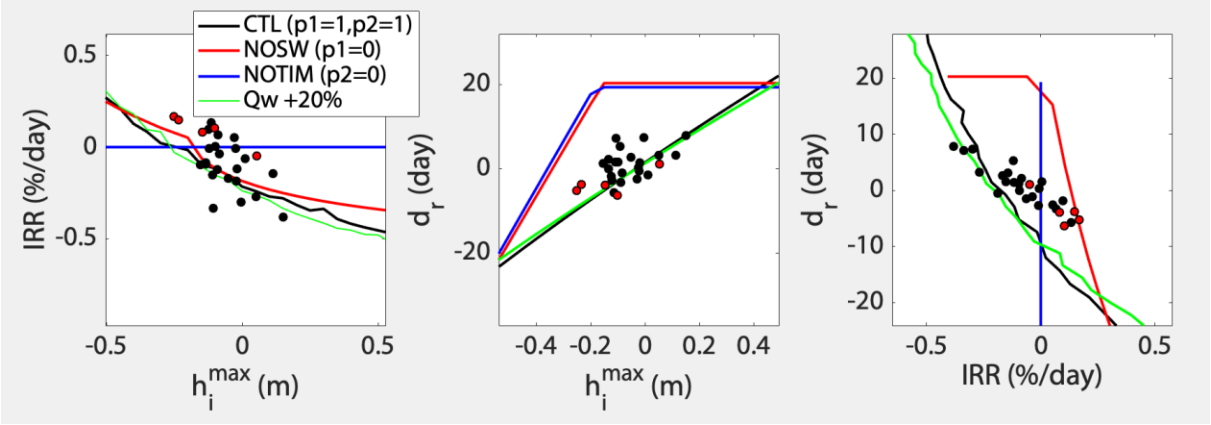

Figure A2. Model (lines) versus observed (symbols) relationships between h_{max}, *IRR* and d_r. The CTL model ensemble (black) has all processes included as described above. The red ensemble assumes SW absorption is fixed at initial value (p_1=0, corresponding to A = 0.99). The blue ensemble assumes concentration does not decrease upon thickness decrease (p_2=0). The green ensemble has 20% larger ocean sensible heat flux. The last five years of observations are highlighted in red.

Second, relationships between observed anomalies (same data as in Figure 4 and 7) and the control ensemble (black) are compatible. Indeed, we get roughly linear relationships over the observed range of variations and slopes are compatible with observations. However, observations differ from the model in two ways. There is spread in the observations, which reflects the presence of non-ideal, non-thermodynamic drivers. Additionally, the retreat date is less sensitive to removal rate in observations than in model.

Third, the IAF is key to establish the relationships between h_{max}, *IRR* and d_r, sensitivity ensembles show. Indeed, with no loss of concentration upon basal melt (blue), the removal rate does not vary. Also, with prescribed solar absorption efficiency (red), the *IRR* vs h_{max} relationship is preserved and the latter is set by concentration loss rate (see Equation (A. 2)). Retreat occurs later, but the rate of change in retreat date per unit of thickness or IRR is large.

C.4 Conclusions

The observed behavior with linearly co-evolving h_{max}, *IRR* and d_r are compatible with a thermodynamic response to sea ice thinning. The ice albedo feedback seems a key driver of the observed changes. In particular, observed changes in IRR are characteristic of the ice-albedo-feedback as conceptualized by Holland et al. (2006), connecting solar radiation absorption through open water, basal melt of thin ice concentration loss.

Acknowledgments

This research has been funded by the SCAR INSTANT research programme.

Data Availability

The present analyses are based on publicly available observational data. OSI-SAF sea ice concentration and drift are available from https://osi-saf.eumetsat.int/products. ESA CCI sea surface temperature is available from https://cds.climate.copernicus.eu/cdsapp#!/home. Sea ice thickness data is available from https://zenodo.org/records/10610697.

Competing Interests Statement

The authors declare no competing interests.

References

Behrendt, A., Dierking, W., Fahrbach, E., & Witte, H. (2013). Sea ice draft in the Weddell Sea, measured by upward looking sonars. *Earth System Science Data*, *5*(1), 209-226. https://doi.org/10.5194/essd-5-209-2013

Bocquet, M. (2023). *Arctic and Antarctic sea ice volume changes estimation from satellite altimetry between 1994 ans 2023*.

Bocquet, M., & Fleury, S. (2024). *Antarctic sea ice thickness climate data record (ERS-1, ERS-2, Envisat, CryoSat-2) using a snow depth climatology* [jeu de données]. Zenodo. https://doi.org/10.5281/zenodo.10610697

Burt, M. A., Randall, D. A., & Branson, M. D. (2016). Dark Warming. *Journal of Climate*, *29*(2), 705-719. https://doi.org/10.1175/JCLI-D-15-0147.1

Cavalieri, D. J., & Parkinson, C. L. (2012). Arctic sea ice variability and trends, 1979–2010. *The Cryosphere*, *6*(4), 881-889. https://doi.org/10.5194/tc-6-881-2012

Clem, K. R., & Fogt, R. L. (2015). South Pacific circulation changes and their connection to the tropics and regional Antarctic warming in austral spring, 1979–2012. *Journal of Geophysical Research: Atmospheres*, *120*(7), 2773-2792. https://doi.org/10.1002/2014JD022940

Comiso, J. (2017). *Bootstrap Sea Ice Concentrations from Nimbus-7 SMMR and DMSP SSM/I-SSMIS Passive Microwave Data, Version 3*. https://doi.org/10.5067/7Q8HCCWS4I0R

Ferreira, D., Marshall, J., Bitz, C. M., Solomon, S., & Plumb, A. (2015). Antarctic Ocean and Sea Ice Response to Ozone Depletion : A Two-Time-Scale Problem. *Journal of Climate*, *28*(3), 1206-1226. https://doi.org/10.1175/JCLI-D-14-00313.1

Fichefet, T., & Morales Maqueda, M. A. (1997). Sensitivity of a global sea ice model to the treatment of ice thermodynamics and dynamics. *Journal of Geophysical Research*, *102*, 12,609-12,646.

Gordon, A. L. (1981). Seasonality of Southern Ocean sea ice. *Journal of Geophysical Research: Oceans*, *86*(C5), 4193-4197. https://doi.org/10.1029/JC086iC05p04193

Guo, Y., Chen, X., Huang, S., & Wen, Z. (2023). Amplified Interannual Variation of the Summer Sea Ice in the Weddell Sea, Antarctic After the Late 1990s. *Geophysical Research Letters*, *50*(17), e2023GL104924. https://doi.org/10.1029/2023GL104924

Häkkinen, S., & Mellor, G. L. (1990). One hundred years of Arctic ice cover variations as simulated by a one-dimensional, ice-ocean model. *Journal of Geophysical Research: Oceans*, *95*(C9), 15959-15969. https://doi.org/10.1029/JC095iC09p15959

Haumann, F. A., Moorman, R., Riser, S. C., Smedsrud, L. H., Maksym, T., Wong, A. P. S., Wilson, E. A., Drucker, R., Talley, L. D., Johnson, K. S., Key, R. M., & Sarmiento, J. L. (2020). Supercooled Southern Ocean Waters. *Geophysical Research Letters*, *47*(20), e2020GL090242. https://doi.org/10.1029/2020GL090242

Hersbach, H., Bell, B., Berrisford, P., Hirahara, S., Horányi, A., Muñoz-Sabater, J., Nicolas, J., Peubey, C., Radu, R., Schepers, D., Simmons, A., Soci, C., Abdalla, S., Abellan, X., Balsamo, G., Bechtold, P., Biavati, G., Bidlot, J., Bonavita, M., … Thépaut, J.-N. (2020). The ERA5 global reanalysis. *Quarterly Journal of the Royal Meteorological Society*, *146*(730), 1999-2049. https://doi.org/10.1002/qj.3803

Himmich, K., Vancoppenolle, M., Madec, G., Sallée, J.-B., Holland, P. R., & Lebrun, M. (2023). Drivers of Antarctic sea ice advance. *Nature Communications*, *14*(1), Article 1. https://doi.org/10.1038/s41467-023-41962-8

Holland, M. M., Bitz, C. M., Hunke, E. C., Lipscomb, W. H., & Schramm, J. L. (2006). Influence of the Sea Ice Thickness Distribution on Polar Climate in CCSM3. *Journal of Climate*, *19*(11), 2398-2414. https://doi.org/10.1175/JCLI3751.1

Holland, M. M., Blanchard-Wrigglesworth, E., Kay, J., & Vavrus, S. (2013). Initial-value predictability of Antarctic sea ice in the Community Climate System Model 3. *Geophysical Research Letters*, *40*(10), 2121-2124. https://doi.org/10.1002/grl.50410

Holland, M. M., Landrum, L., Raphael, M., & Stammerjohn, S. (2017). Springtime winds drive Ross Sea ice variability and change in the following autumn. *Nature Communications*, *8*(1), Article 1. https://doi.org/10.1038/s41467-017-00820-0

Holland, P. R., & Kimura, N. (2016). Observed Concentration Budgets of Arctic and Antarctic Sea Ice. *Journal of Climate*, *29*(14), 5241-5249. https://doi.org/10.1175/JCLI-D-16-0121.1

Holland, P. R., & Kwok, R. (2012). Wind-driven trends in Antarctic sea-ice drift. *Nature Geoscience*, *5*(12), Article 12. https://doi.org/10.1038/ngeo1627

Kimura, N., Onomura, T., & Kikuchi, T. (2023). Processes governing seasonal and interannual change of the Antarctic sea-ice area. *Journal of Oceanography*, *79*(2), 109-121. https://doi.org/10.1007/s10872-022-00669-y

Kostov, Y., Marshall, J., Hausmann, U., Armour, K. C., Ferreira, D., & Holland, M. M. (2017). Fast and slow responses of Southern Ocean sea surface temperature to SAM in coupled climate models. *Climate Dynamics*, *48*(5), 1595-1609. https://doi.org/10.1007/s00382-016-3162-z

Kurtz, N. T., Farrell, S. L., Studinger, M., Galin, N., Harbeck, J. P., Lindsay, R., Onana, V. D., Panzer, B., & Sonntag, J. G. (2013). Sea ice thickness, freeboard, and snow depth products from Operation IceBridge airborne data. *The Cryosphere*, *7*(4), 1035-1056. https://doi.org/10.5194/tc-7-1035-2013

Kurtz, N. T., & Markus, T. (2012). Satellite observations of Antarctic sea ice thickness and volume. *Journal of Geophysical Research: Oceans*, *117*(C8). https://doi.org/10.1029/2012JC008141

Lavergne, T., & Down, E. (2023). A Climate Data Record of Year-Round Global Sea Ice Drift from the EUMETSAT OSI SAF. *Earth System Science Data Discussions*, 1-38. https://doi.org/10.5194/essd-2023-40

Lavergne, T., Sørensen, A. M., Kern, S., Tonboe, R., Notz, D., Aaboe, S., Bell, L., Dybkjær, G., Eastwood, S., Gabarro, C., Heygster, G., Killie, M. A., Brandt Kreiner, M., Lavelle, J., Saldo, R., Sandven, S., & Pedersen, L. T. (2019). Version 2 of the EUMETSAT OSI SAF and ESA CCI sea-ice concentration climate data records. *The Cryosphere*, *13*(1), 49-78. https://doi.org/10.5194/tc-13-49-2019

Laxon, S., Peacock, N., & Smith, D. (2003). High interannual variability of sea ice thickness in the Arctic region. *Nature*, *425*, 947-950.

Lebrun, M., Vancoppenolle, M., Madec, G., & Massonnet, F. (2019). Arctic sea-ice-free season projected to extend into autumn. *The Cryosphere*, *13*(1), 79-96. https://doi.org/10.5194/tc-13-79-2019

Lengaigne, M., Menkes, C., Aumont, O., Gorgues, T., Bopp, L., André, J.-M., & Madec, G. (2007). Influence of the oceanic biology on the tropical Pacific climate in a coupled general circulation model. *Climate Dynamics*, *28*(5), 503-516. https://doi.org/10.1007/s00382-006-0200-2

Liao, S., Luo, H., Wang, J., Shi, Q., Zhang, J., & Yang, Q. (2022). An evaluation of Antarctic sea-ice thickness from the Global Ice-Ocean Modeling and Assimilation System based on in situ and satellite observations. *The Cryosphere*, *16*(5), 1807-1819. https://doi.org/10.5194/tc-16-1807-2022

Libera, S., Hobbs, W., Klocker, A., Meyer, A., & Matear, R. (2022). Ocean-Sea Ice Processes and Their Role in Multi-Month Predictability of Antarctic Sea Ice. *Geophysical Research Letters*, *49*(8), e2021GL097047. https://doi.org/10.1029/2021GL097047

Maksym, T., & Markus, T. (2008). Antarctic Sea Ice Thickness and Snow-to-Ice Conversion from Atmospheric Reanalysis and Passive Microwave Snow Depth. *Journal of Geophysical Research*, *113*.

https://doi.org/10.1029/2006JC004085
Mallett, R. D. C., Lawrence, I. R., Stroeve, J. C., Landy, J. C., & Tsamados, M. (2020). Brief communication : Conventional assumptions involving the speed of radar waves in snow introduce systematic underestimates to sea ice thickness and seasonal growth rate estimates. *The Cryosphere*, *14*(1), 251-260. https://doi.org/10.5194/tc-14-251-2020
Martinson, D. G., & Iannuzzi, R. A. (1998). Antarctic Ocean-Ice Interaction : Implications from Ocean Bulk Property Distributions in the Weddell Gyre. In *Antarctic Sea Ice : Physical Processes, Interactions and Variability* (p. 243-271). American Geophysical Union (AGU). https://doi.org/10.1029/AR074p0243
Massom, R. A., Stammerjohn, S. E., Lefebvre, W., Harangozo, S. A., Adams, N., Scambos, T. A., Pook, M. J., & Fowler, C. (2008). West Antarctic Peninsula sea ice in 2005 : Extreme ice compaction and ice edge retreat due to strong anomaly with respect to climate. *Journal of Geophysical Research: Oceans*, *113*(C2). https://doi.org/10.1029/2007JC004239
Maykut, G. A., & McPhee, M. G. (1995). Solar heating of the Arctic mixed layer. *Journal of Geophysical Research: Oceans*, *100*(C12), 24691-24703. https://doi.org/10.1029/95JC02554
Maykut, G. A., & Perovich, D. K. (1987). The role of shortwave radiation in the summer decay of a sea ice cover. *Journal of Geophysical Research: Oceans*, *92*(C7), 7032-7044. https://doi.org/10.1029/JC092iC07p07032
Meehl, G. A., Arblaster, J. M., Bitz, C. M., Chung, C. T. Y., & Teng, H. (2016). Antarctic sea-ice expansion between 2000 and 2014 driven by tropical Pacific decadal climate variability. *Nature Geoscience*, *9*(8), Article 8. https://doi.org/10.1038/ngeo2751
Meehl, G. A., Arblaster, J. M., Chung, C. T. Y., Holland, M. M., DuVivier, A., Thompson, L., Yang, D., & Bitz, C. M. (2019). Sustained ocean changes contributed to sudden Antarctic sea ice retreat in late 2016. *Nature Communications*, *10*(1), Article 1. https://doi.org/10.1038/s41467-018-07865-9
Merchant, C. J., Embury, O., Bulgin, C. E., Block, T., Corlett, G. K., Fiedler, E., Good, S. A., Mittaz, J., Rayner, N. A., Berry, D., Eastwood, S., Taylor, M., Tsushima, Y., Waterfall, A., Wilson, R., & Donlon, C. (2019). Satellite-based time-series of sea-surface temperature since 1981 for climate applications. *Scientific Data*, *6*(1), Article 1. https://doi.org/10.1038/s41597-019-0236-x
Parkinson, C. L. (1994). Spatial patterns in the length of the sea ice season in the Southern Ocean, 1979–1986. *Journal of Geophysical Research: Oceans*, *99*(C8), 16327-16339. https://doi.org/10.1029/94JC01146
Parkinson, C. L. (2019). A 40-y record reveals gradual Antarctic sea ice increases followed by decreases at rates far exceeding the rates seen in the Arctic. *Proceedings of the National Academy of Sciences*, *116*(29), 14414-14423. https://doi.org/10.1073/pnas.1906556116
Parkinson, C. L., & Cavalieri, D. J. (2012). Antarctic sea ice variability and trends, 1979–2010. *The Cryosphere*, *6*(4), 871-880. https://doi.org/10.5194/tc-6-871-2012
Paul, S., Sallila, H, Hendricks, S., & Rinne, E. (2021). *ESA CCI+ Climate Change Initiative Phase 1, D2.1 Sea Ice Thickness Algorithm Theoretical Basis Document (ATBD), v.3.1*. https://climate.esa.int/en/projects/sea-ice/Sea-Ice-Key-Documents/
Perovich, D. K., Light, B., Eicken, H., Jones, K. F., Runciman, K., & Nghiem, S. V. (2007). Increasing solar heating of the Arctic Ocean and adjacent seas, 1979–2005 : Attribution and role in the ice-albedo feedback. *Geophysical Research Letters*, *34*(19). https://doi.org/10.1029/2007GL031480
Purich, A., & Doddridge, E. W. (2023). Record low Antarctic sea ice coverage indicates a new sea ice state. *Communications Earth & Environment*, *4*(1), Article 1. https://doi.org/10.1038/s43247-023-00961-9
Raphael, M. N., & Handcock, M. S. (2022). A new record minimum for Antarctic sea ice. *Nature Reviews Earth & Environment*, *3*(4), Article 4. https://doi.org/10.1038/s43017-022-00281-0
Saenz, B. T., McKee, D. C., Doney, S. C., Martinson, D. G., & Stammerjohn, S. E. (2023). Influence of seasonally varying sea-ice concentration and subsurface ocean heat on sea-ice thickness and sea-ice seasonality for a 'warm-shelf' region in Antarctica. *Journal of Glaciology*, *69*(277), 1466-1482. https://doi.org/10.1017/jog.2023.36
Schlosser, E., Haumann, F. A., & Raphael, M. N. (2018). Atmospheric influences on the anomalous 2016 Antarctic sea ice decay. *The Cryosphere*, *12*(3), 1103-1119. https://doi.org/10.5194/tc-12-1103-2018
Schroeter, S., O'Kane, T. J., & Sandery, P. A. (2023). Antarctic sea ice regime shift associated with decreasing zonal symmetry in the Southern Annular Mode. *The Cryosphere*, *17*(2), 701-717. https://doi.org/10.5194/tc-17-701-2023
Simpkins, G. R., Ciasto, L. M., & England, M. H. (2013). Observed variations in multidecadal Antarctic sea ice trends during 1979–2012. *Geophysical Research Letters*, *40*(14), 3643-3648. https://doi.org/10.1002/grl.50715
Smith, A., Jahn, A., & Wang, M. (2020). Seasonal transition dates can reveal biases in Arctic sea ice simulations. *The Cryosphere*, *14*(9), 2977-2997. https://doi.org/10.5194/tc-14-2977-2020
Stammerjohn, S. E., Martinson, D. G., Smith, R. C., Yuan, X., & Rind, D. (2008). Trends in Antarctic annual sea ice

retreat and advance and their relation to El Niño–Southern Oscillation and Southern Annular Mode variability. *Journal of Geophysical Research: Oceans*, *113*(C3). https://doi.org/10.1029/2007JC004269

Stammerjohn, S., Massom, R., Rind, D., & Martinson, D. (2012). Regions of rapid sea ice change : An inter-hemispheric seasonal comparison. *Geophysical Research Letters*, *39*(6). https://doi.org/10.1029/2012GL050874

Stuecker, M. F., Bitz, C. M., & Armour, K. C. (2017). Conditions leading to the unprecedented low Antarctic sea ice extent during the 2016 austral spring season. *Geophysical Research Letters*, *44*(17), 9008-9019. https://doi.org/10.1002/2017GL074691

Turner, J., Holmes, C., Caton Harrison, T., Phillips, T., Jena, B., Reeves-Francois, T., Fogt, R., Thomas, E. R., & Bajish, C. C. (2022). Record Low Antarctic Sea Ice Cover in February 2022. *Geophysical Research Letters*, *49*(12), e2022GL098904. https://doi.org/10.1029/2022GL098904

Turner, J., Phillips, T., Marshall, G. J., Hosking, J. S., Pope, J. O., Bracegirdle, T. J., & Deb, P. (2017). Unprecedented springtime retreat of Antarctic sea ice in 2016. *Geophysical Research Letters*, *44*(13), 6868-6875. https://doi.org/10.1002/2017GL073656

Vancoppenolle, M., Timmermann, R., Ackley, S. F., Fichefet, T., Goosse, H., Heil, P., Lieser, J., Leonard, K. C., M. Nicolaus, Papakyriakou, T., & Tison, J.-L. (2011). Assessment of radiation forcing data sets for large-scale sea ice models in the Southern Ocean. *Deep Sea Research (II)*, *58*, 1237-1249. https://doi.org/10.1016/j.dsr2.2010.10.039

Vivier, F., Hutchings, J. K., Kawaguchi, Y., Kikuchi, T., Morison, J. H., Lourenço, A., & Noguchi, T. (2016). Sea ice melt onset associated with lead opening during the spring/summer transition near the North Pole. *Journal of Geophysical Research: Oceans*, *121*(4), 2499-2522. https://doi.org/10.1002/2015JC011588

Wilson, E. A., Riser, S. C., Campbell, E. C., & Wong, A. P. S. (2019). Winter Upper-Ocean Stability and Ice–Ocean Feedbacks in the Sea Ice–Covered Southern Ocean. *Journal of Physical Oceanography*, *49*(4), 1099-1117. https://doi.org/10.1175/JPO-D-18-0184.1

Worby, A. P., Geiger, C. A., Paget, M. J., Van Woert, M. L., Ackley, S. F., & DeLiberty, T. L. (2008). Thickness distribution of Antarctic sea ice. *Journal of Geophysical Research: Oceans*, *113*(C5). https://doi.org/10.1029/2007JC004254

Zhang, L., Delworth, T. L., Yang, X., Zeng, F., Lu, F., Morioka, Y., & Bushuk, M. (2022). The relative role of the subsurface Southern Ocean in driving negative Antarctic Sea ice extent anomalies in 2016–2021. *Communications Earth & Environment*, *3*(1), Article 1. https://doi.org/10.1038/s43247-022-00624-1